International Communications in Heat and Mass Transfer 38 (2011) 368–376

Contents lists available at ScienceDirect

International Communications in Heat and Mass Transfer

journal homepage: www.elsevier.com/locate/ichmt

Natural convection in porous triangular enclosure with a centered conducting body ☆

Yasin Varol *

Department of Mechanical Education, Firat University, 23119 Elazig, Turkey

ARTICLE INFO

Available online 21 December 2010

Keywords:
Porous media
Conducting body
Triangular enclosure

ABSTRACT

A numerical work was performed to examine the heat transfer and fluid flow due to natural convection in a porous triangular enclosure with a centered conducting body. The center of the body was located onto the gravity center of the right-angle triangular cavity. The Darcy law model was used to write the governing equations and they were solved using a finite difference method. Results are presented by streamlines, isotherms, mean and local Nusselt numbers for the different parameters such as the Rayleigh number, thermal conductivity ratio, and height and width of the body. It was observed that both height and width of the body and thermal conductivity ratio play an important role on heat and fluid flow inside the cavity.

1. Introduction

Porous media filled enclosures or channels were an important subject of engineering. It had very wide application areas such as solar collection, building insulation, oil distraction, building materials and some geophysical or geological applications. Analysis of the flow field and temperature distribution was also a topic in applied mathematics. All of these were given in literature on porous media [1–4].

Natural convection in a triangular shaped enclosure was mostly studied for a pure fluid filled enclosure due to its wide application for roof-building, electronic equipment and some solar applications [5–9].

Porous media filled attic shaped building was firstly proposed by Poulikakos and Bejan [10]. They proposed that the filling of attic shaped building with porous media can be a control element for heat transfer and fluid flow. Varol et al. [11] made a numerical work on natural convection in porous media filled right-angle triangular enclosure by adding a square object at different thermal boundary conditions. In this article, they indicated that thermal conditions play an important role on heat and fluid flow. Inserting of a passive element into a cavity or pipe was an old technique to control heat transfer and fluid flow of pure fluid or fluid saturated porous media. In this context, Dong and Li [12] made a numerical work to investigate the complicated flow and heat transfer phenomena in a circle shaped body inserted thick walled enclosure. Ha et al. [13] tested the different boundary conditions for the inserted body to the enclosure. They reported that the presence of the body obstructs the flow and temperature fields. Other related articles can be found in Refs. [14–16].

The main purpose of this work was to evaluate the dimensions and thermal conductivity ratio of a body in porous media filled triangular enclosures. Based on the previously mentioned literature survey and the authors' knowledge there is no study in literature for considered geometry.

2. Analysis

The schematic of the geometry with the coordinates and boundary conditions is shown in Fig. 1(a). The problem was considered to be two dimensional. The vertical wall was insulated. The bottom wall was maintained at a constant high temperature of T_h whereas the inclined wall was in a constant low temperature of T_c. A conducting body with height wy', and width wx' was inserted to the center of the enclosure. Its coordinate was $cx'$and cy'. The conducting body was located far from the origin with the distance of 0.33 in both directions ($cx' = cy' = 0.33$). L and H represented the bottom length and the height of the vertical wall, respectively. Thus, an aspect ratio was defined as H/L which was taken as unity in this paper. The grid distribution is also shown in Fig. 1(b). A regular grid was used in the system.

The following assumptions are made to obtain the governing equations: the properties of the fluid and the porous medium are constant; the cavity walls are impermeable; the Boussinesq approximation and the Darcy law model are valid; and the viscous drag and inertia terms of the momentum equations are negligible. With these assumptions, the dimensional governing equations of continuity, momentum, and energy can be written as

$$\frac{\partial u}{\partial x} + \frac{\partial v}{\partial y} = 0 \tag{1}$$

$$\frac{\partial u}{\partial y} - \frac{\partial v}{\partial x} = -\frac{g\beta K}{\upsilon}\frac{\partial T_f}{\partial x} \tag{2}$$

$$u\frac{\partial T_f}{\partial x} + v\frac{\partial T_f}{\partial y} = \alpha_m\left(\frac{\partial^2 T_f}{\partial x^2} + \frac{\partial^2 T_f}{\partial y^2}\right) \tag{3}$$

☆ Communicated by W.J. Minkowycz.

* Corresponding author.
E-mail address: ysnvarol@gmail.com.

0735-1933/$ – see front matter © 2010 Elsevier Ltd. All rights reserved.
doi:10.1016/j.icheatmasstransfer.2010.12.013

Nomenclature

cx'	location of the conducting body in $x-$direction
cy'	location of the conducting body in $y-$direction
g	gravitational acceleration
H	height of the triangle or cavity
k	thermal conductivity ratio, k_s/k_f
K	permeability of the porous medium
L	length of the triangle or cavity
Nu	mean Nusselt number
Nu_x	local Nusselt number
Ra	Rayleigh number
T	temperature
$u,\ v$	velocity components in x,y directions
x,y	Cartesian coordinates
wx	dimensionless width of the conducting body, wx'/L
wy	dimensionless height of the conducting body, wy'/H

Greek Letters

α_m	thermal diffusivity of the porous medium
β	thermal expansion coefficient
θ	non-dimensional temperature
υ	kinematic viscosity
ψ	stream function
Ψ	non-dimensional stream function

Subscript

c	cold
f	fluid
h	hot
s	solid

for the fluid-saturated porous medium and the energy equation for the body wall is given by:

$$\frac{\partial^2 T_s}{\partial x^2}+\frac{\partial^2 T_s}{\partial y^2}=0 \tag{4}$$

where u and v are the velocity components along the x and y axes, T_f is the fluid temperature, g is the acceleration due to gravity, T_s is the temperature of the body wall, K is the permeability of the porous medium, α_m is the effective thermal diffusivity of the porous medium, β is the thermal expansion coefficient and υ is the kinematic viscosity. Introducing the stream function ψ defined as

$$u=\frac{\partial\psi}{\partial y},\qquad v=-\frac{\partial\psi}{\partial x} \tag{5}$$

Eqs. (1)–(4) can be written in non-dimensional form as

$$\frac{\partial^2\Psi}{\partial X^2}+\frac{\partial^2\Psi}{\partial Y^2}=-Ra\frac{\partial\theta_f}{\partial X} \tag{6}$$

$$\frac{\partial\Psi}{\partial Y}\frac{\partial\theta_f}{\partial X}-\frac{\partial\Psi}{\partial X}\frac{\partial\theta_f}{\partial Y}=\frac{\partial^2\theta_f}{\partial X^2}+\frac{\partial^2\theta_f}{\partial Y^2} \tag{7}$$

for the fluid-saturated porous medium and

$$\frac{\partial^2\theta_s}{\partial X^2}+\frac{\partial^2\theta_s}{\partial Y^2}=0 \tag{8}$$

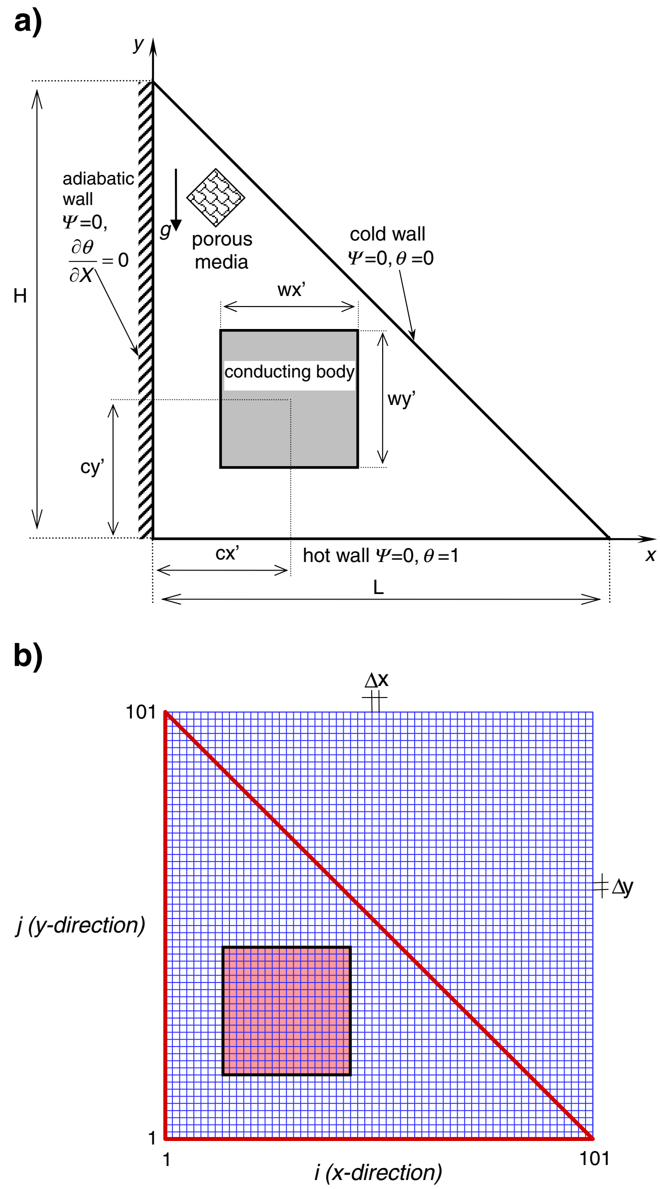

Fig. 1. a) Physical model, b) Finite-difference grid for a triangular enclosure.

for the body wall, respectively. Here $Ra=g\beta K(T_h-T_c)H/\alpha_m\upsilon$ is the Rayleigh number for the porous medium and the non-dimensional quantities are defined as

$$X=\frac{x}{H},\ Y=\frac{y}{H},\ \Psi=\frac{\psi}{\alpha_m},\quad \theta_f=\frac{T_f-T_c}{T_h-T_c},\ \theta_s=\frac{T_s-T_c}{T_h-T_c} \tag{9}$$

The boundary conditions of Eqs. (6)–(8) are:for all solid boundaries

$$\Psi=0 \tag{10a}$$

on the bottom wall (hot), $0\le X\le 1$

$$\theta_f=1 \tag{10b}$$

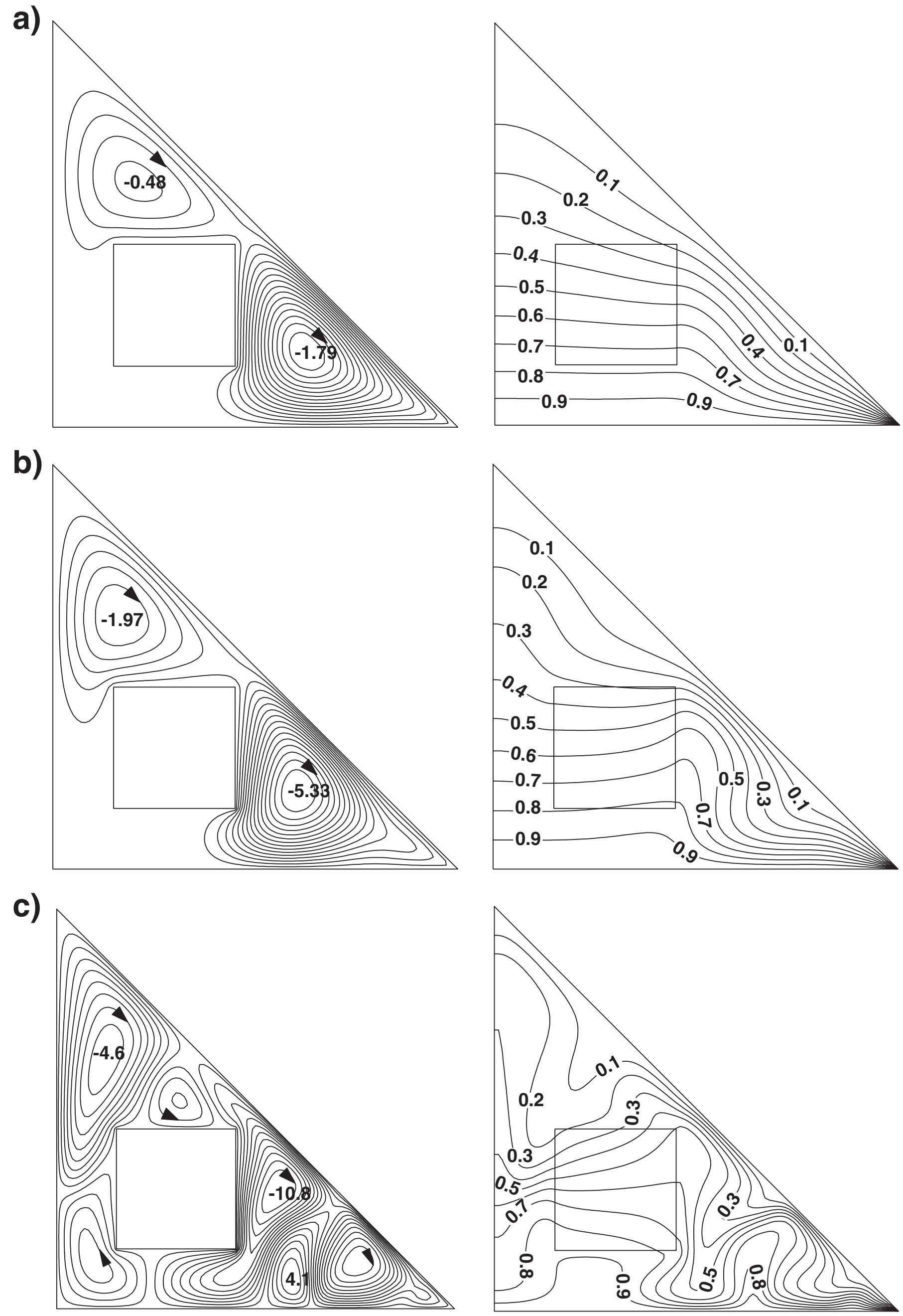

Fig. 2. Streamlines (left) and isotherms (right) for different Rayleigh numbers at $wx = 0.3$, $wy = 0.3$, and $k = 1$: a) $Ra = 100$, b) $Ra = 250$, c) $Ra = 1000$.

on the vertical wall (adiabatic), $0 \leq Y \leq 1$

$$\frac{\partial \theta_f}{\partial X} = 0 \tag{10c}$$

on the inclined wall (cold)

$$\theta_f = 0 \tag{10d}$$

for the interface between solid and porous media,

$$k_f \frac{\partial \theta_f}{\partial n} = k_s \frac{\partial \theta_s}{\partial n} \tag{10e}$$

Physical quantities of interest in this problem are the local Nusselt number Nu_x and the mean Nusselt number Nu, which can be expressed as

$$Nu_x = \left(-\frac{\partial \theta_f}{\partial Y} \right)_{Y=0}, \quad Nu = \int_0^1 Nu_x dX \tag{11a, b}$$

Eqs. (6)–(8) subject to the boundary conditions (10) were integrated using the finite-difference method. Numerical simulations were carried out systematically in order to determine the effect of three main parameters of the problem, namely: Rayleigh number Ra, thermal conductivity ratio k, width of the conducting body $wx(= wx'/L)$and height of the conducting body $wy(= wy'/H)$ on the flow and heat transfer characteristics. The solution domain, therefore, consists of grid

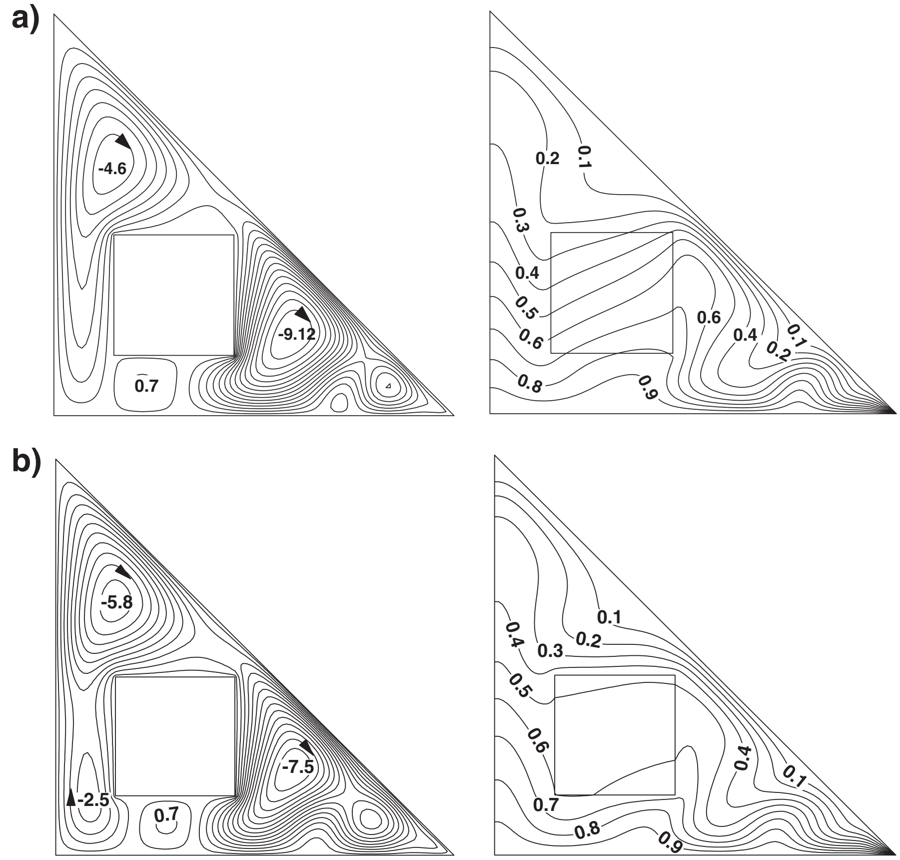

Fig. 3. Streamlines (left) and isotherms (right) for different thermal conductivity ratios at $wx = 0.3$, $wy = 0.3$, and $Ra = 500$: a) $k = 1$, b) $k = 10$.

points at which equations were applied. The grid size was selected to be similar to that used by 101×101 for the triangular cavity with uniform grid spacing. The resulting algebraic equations were solved by Successive under Relaxation (SUR) method. The iteration process was terminated under the following condition:

$$\sum_{i,j} \left| \frac{\phi_{i,j}^{m} - \phi_{i,j}^{m-1}}{\phi_{i,j}^{m}} \right| \le 10^{-5} \tag{12}$$

where m denoted the iteration step and ϕ stands for either θ_f, θ_s or Ψ. Due to lack of suitable results in the literature pertaining to the present configuration, the obtained results have been validated against the existing results for a square cavity filled with a porous medium. Thus, the comparison of the present results for the mean Nusselt number Nu, as defined by Eq. (11a,b), with those from the open literature has been made for a value of $Ra = 1000$. Comparison results can be found in our earlier publications as Varol et al. [16].

3. Results and discussion

In this numerical study, buoyancy induced flow due to temperature difference in a closed triangular cavity with solid conductive body inserted was analyzed through a computer code written by the author. Results are presented by streamlines, isotherms, mean and local Nusselt numbers for the different parameters such as the Rayleigh number, thermal conductivity ratio, height and width of the body.

Fig. 2(a) to (c) illustrates the effects of the Rayleigh number on heat and fluid flow in a square shaped solid body inserted. For all studies, the center of the body sits in the gravity center of the triangular enclosure. In this case, thermal conductivity values of solid and fluid are equal to each other. Thus, thermal conductivity ratio is taken as unity. In Fig. 2(a), two eddies were formed near the right bottom corner of the triangle and top of the square body. The flow strength ($\Psi_{\min} = -1.79$) was higher near the right bottom corner due to a high temperature difference between the hot and cold surfaces and the small distance between them. Both eddies turned in the same clockwise direction. Due to the low values of the Rayleigh number, the conduction mode of heat transfer became dominant onto convection. Thus, insertion of the square body does not make a strong effect on temperature distribution as shown in Fig. 2(a). This is due to the fact that the thermal conductivity ratio is equal to unity. Further Rayleigh numbers show that the direction of temperature distribution changes due to the presence of the body as given in Fig. 2(b) to (c). For the highest value of the Rayleigh number, multiple eddies were observed. For a higher value than $Ra = 1000$, two dimensional and steady state solution may not be enough to obtain heat and fluid flow in the same system. Thus, the Rayleigh number is restricted in this work.

Fig. 3(a) to (b) illustrates the streamline and isotherms for $Ra = 500$ and high thermal conductivity ratio as $k = 1$ and $k = 10$. Multiple cells were observed for all values of thermal conductivity. However, only the eddy at the right bottom corner was affected from this change. It was seen that the body made small effects on temperature distribution when thermal conductivity ratio became high as given in Fig. 3(b). Effects of the aspect ratio of the inner body is presented in Fig. 4(a) to (c) with streamlines and isotherms for $wx = 0.3$, $wy = 0.3$ and $Ra = 500$. In Fig. 4(a), the horizontal ($wy = 0.2$) and vertical ($wx = 0.2$) rectangular body is inserted. In both cases, multiple cells were observed. As given in Fig. 1 (physical model), the cavity is heated from the bottom side and cooled from the inclined wall. A cell was formed under the inserted body and a higher flow strength was formed when the body was inserted horizontally due to the wide surface. Due to the narrow distance between the inserted body and the vertical wall the fluid was accelerated. Fig. 5 illustrates the variation of the local Nusselt number along the heated wall for different thermal conductivity ratios. In this case, the square shaped body was inserted into the cavity. General observation indicated that

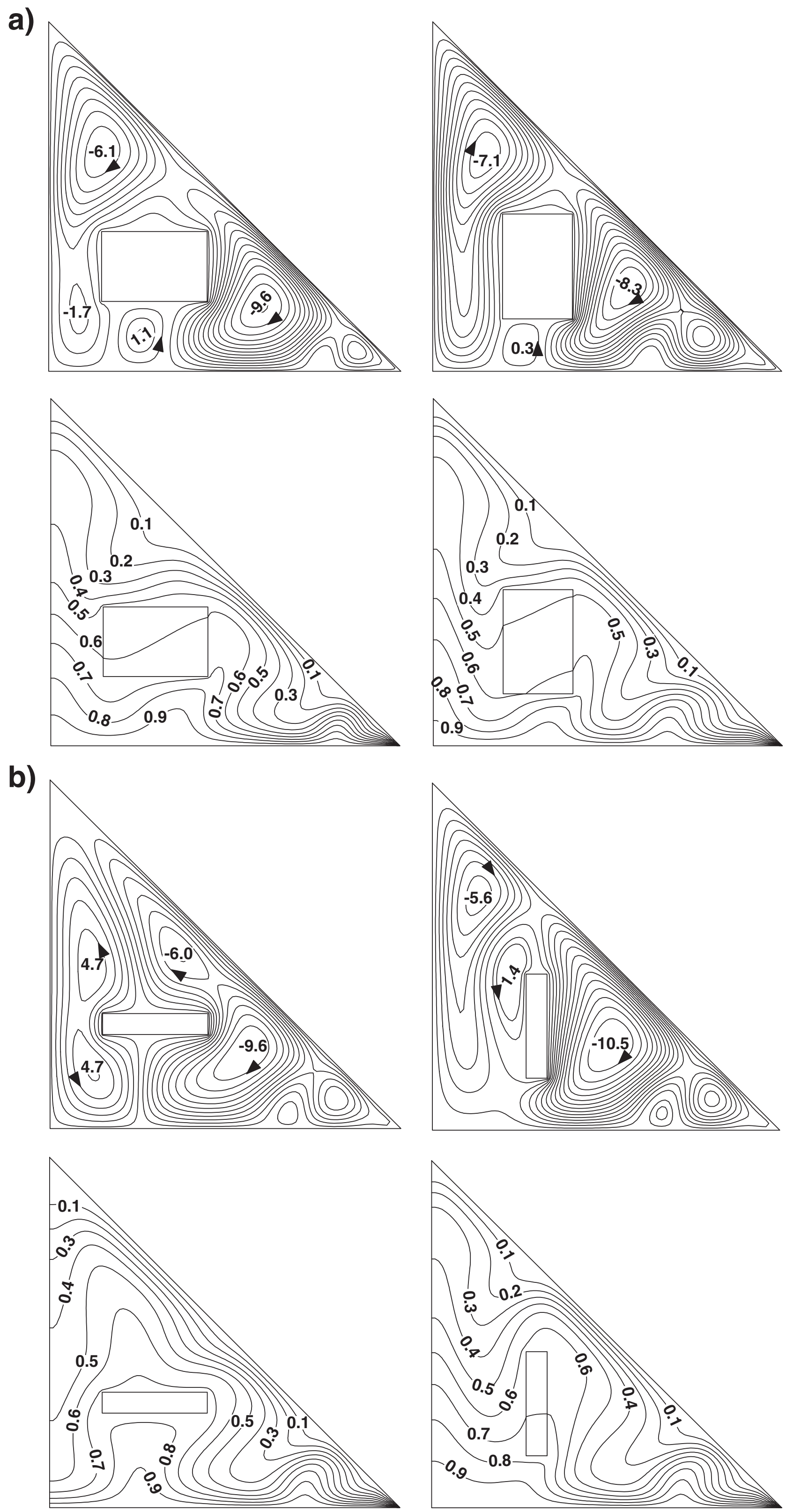

Fig. 4. Streamlines (top) and isotherms (bottom) at $Ra = 500$ for different heights of the conducting body (left) at $wx = 0.3$ and for different widths of the conducting body (right) at $wy = 0.3$: a) $wy = 0.2, wx = 0.2$, b) $wy = 0.05, wx = 0.05$, c) $wy = 0.02, wx = 0.02$.

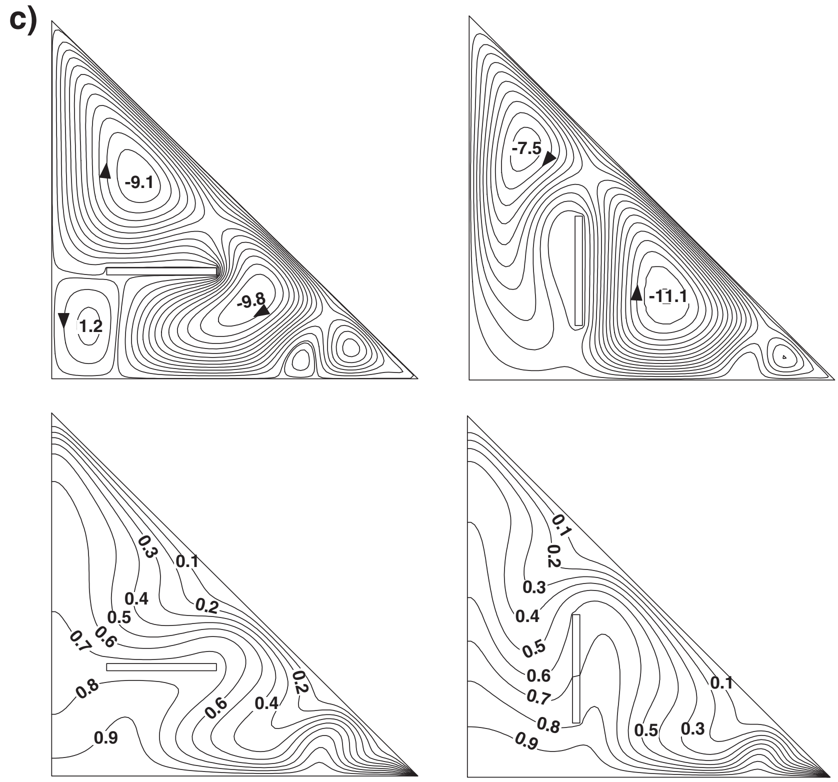

Fig. 4 (*continued*).

heat transfer increases from bottom to top. For $X>0.4$, thermal conductivity ratio became insignificant due to the domination of conduction. Fig. 6(a) and (b) shows the effect of the horizontal and vertical position on the local Nusselt number at $Ra=500$ and $k=1$. As seen from the figure that heat transfer was locally affected from the change of position of the body. It got clear especially at the bottom side of the wall. Heat transfer was first high at the bottom and it had a minimum value between $X=0.2$ and 0.4. However, this minimum point was a function of the shape of the body. The second minimum point occurred around $X=0.8$. Both values of local Nusselt numbers and the location of the minimum point were almost the same except for $wy=0.05$. It was an interesting observation that a similar situation occurred for the vertical position of the body in Fig. 6(b). Fig. 7 was given to summarize these cases. In this figure, the effects of position on the local Nusselt number was presented for $k=0.1$(on the left) and $k=10$(on the right) at $Ra=500$. It was seen that the thickness of the partition was effective on the variation of the local Nusselt numbers. The trend of the local Nusselt number was independent from the variation of the thermal conductivity ratio. In other words, the values of the local Nusselt number had the highest value near $X=1$. At the left corner of the triangle, the local Nusselt number had a higher value when the body was located horizontally for $wx=wy=0.02$ and 0.05. Effects of the thermal conductivity ratio on heat transfer became clearer in Fig. 8. As seen from the figure, a linear increase occurred with the Rayleigh number in terms of heat transfer. It also increased with the increase of the thermal conductivity ratio. Fig. 9 shows the variation of the mean Nusselt number as a function of thermal conductivity ratio and position. In this figure heat transfer increased with increasing thermal conductivity ratio due to increasing heat interaction between solid and fluid. This increase was clear for $k=0.1$ and 1. For further values, heat transfer became constant.

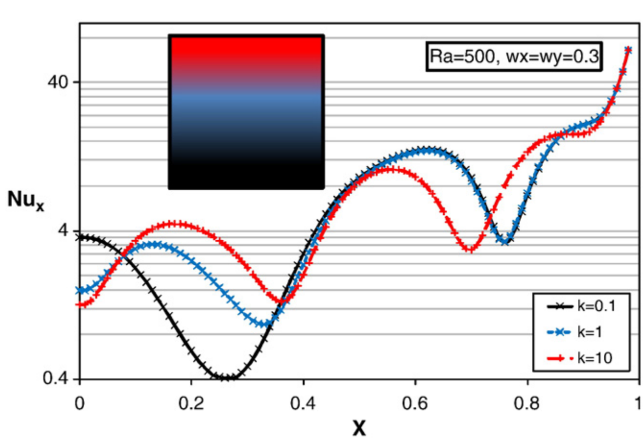

Fig. 5. The variation of the local Nusselt number along the horizontal bottom wall for different thermal conductivity ratios at $Ra=500$,$wx=0.3$, and $wy=0.3$.

4. Conclusions

A numerical work was performed to analyze natural convection in porous media filled and the conducting body inserted triangular cavity. Some findings can be listed as follows:

- Both heat transfer and fluid flow was affected by the location of the conducting body.
- Heat transfer increased with increasing thermal conductivity and Rayleigh number due to incoming energy into the system.
- For a higher value of thermal conductivity, heat transfer became constant. A huge difference occurred between $k=0.1$ and 1on heat transfer.
- Location of the body became more effective than that of thickness of the body.

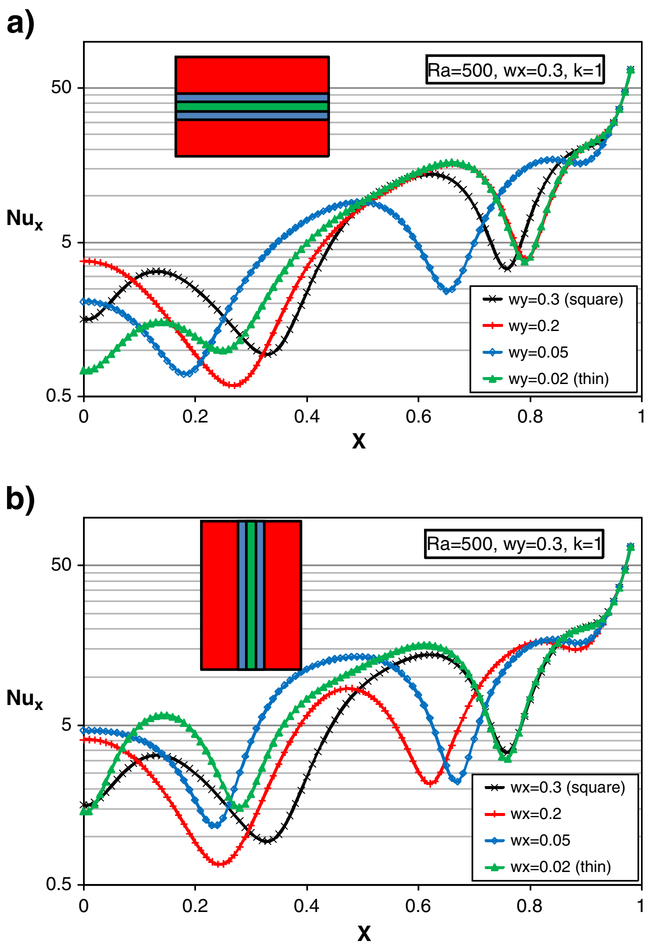

Fig. 6. The variation of the local Nusselt number along the horizontal bottom wall at $k=1$ and $Ra=500$: a) for different heights of the conducting body, b) for different widths of the conducting body.

References

[1] A. Bejan, I. Dincer, S. Lorente, A.F. Miguel, A.H. Reis, Porous and Complex Flow Structures in Modern Technologies, Springer, New York, 2004.

[2] D.B. Ingham, I. Pop (Eds.), Transport phenomena in porous media, vol. III, Elsevier, Oxford, 2005.

[3] D.A. Nield, A. Bejan, Convection in Porous Media, third edSpringer, New York, 2006.

[4] D.B. Ingham, A. Bejan, E. Mamut, I. Pop, Emerging Technologies and Techniques in Porous Media, Kluwer, Dordrecht, 2004.

[5] K. Vafai, Handbook of Porous Media, second ed, Taylor & Francis, New York, 2005.

[6] M.K. Das, K.S.K. Reddy, Conjugate natural convection heat transfer in an inclined square cavity containing a conducting block, Int. J. Heat Mass Transfer 49 (2006) 4987–5000.

[7] J.M. House, C. Beckermann, T.F. Smith, Effect of a centered conducting body on natural convection heat transfer in an enclosure, Numer. Heat Transfer 18 (1990) 213–225.

[8] S.B. Sathe, Y. Joshi, Natural convection arising from a heat generating substrate-mounted protrusion in a liquid-filled two dimensional enclosure, Int. J. Heat Mass Transfer 34 (1991) 2149–2163.

[9] Y.S. Sun, A.F. Amery, Effects of wall conduction, internal heat sources and an internal baffle on natural convection heat transfer in a rectangular enclosure, Int. J. Heat Mass Transfer 40 (1997) 915–929.

[10] D. Poulikakos, A. Bejan, Numerical study of transient high Rayleigh number convection in an attic-shaped porous layer, J. Heat Transfer 105 (1983) 476–484.

[11] Y. Varol, H.F. Oztop, T. Yilmaz, Two-dimensional natural convection in a porous triangular enclosure with a square body, Int. Commun. Heat Mass Transfer 34 (2007) 238–247.

[12] S.F. Dong, Y.T. Li, Conjugate of natural convection and conduction in a complicated enclosure, Int. J. Heat Mass Transfer 47 (2004) 2233–2239.

[13] M.Y. Ha, I.K. Kim, H.S. Yoon, K.S. Yoon, J.R. Lee, S. Balachandar, H.H. Chun, Two-dimensional and unsteady natural convection in a horizontal enclosure with a square body, Numer. Heat Transfer A 41 (2002) 183–210.

[14] Y. Varol, H.F. Oztop, A. Varol, Natural convection in porous triangular enclosures with a solid adiabatic fin attached to the horizontal wall, Int. Commun. Heat Mass Transfer 34 (2007) 19–27.

[15] Y. Varol, A. Koca, H.F. Oztop, Natural convection in a triangle enclosure with flush mounted heater on the wall, Int. Commun. Heat Mass Transfer 33 (2006) 951–958.

[16] Y. Varol, H.F. Oztop, Control of buoyancy-induced temperature and flow fields with an embedded adiabatic thin plate in porous triangular cavities, Appl. Therm. Eng. 29 (2009) 558–566.

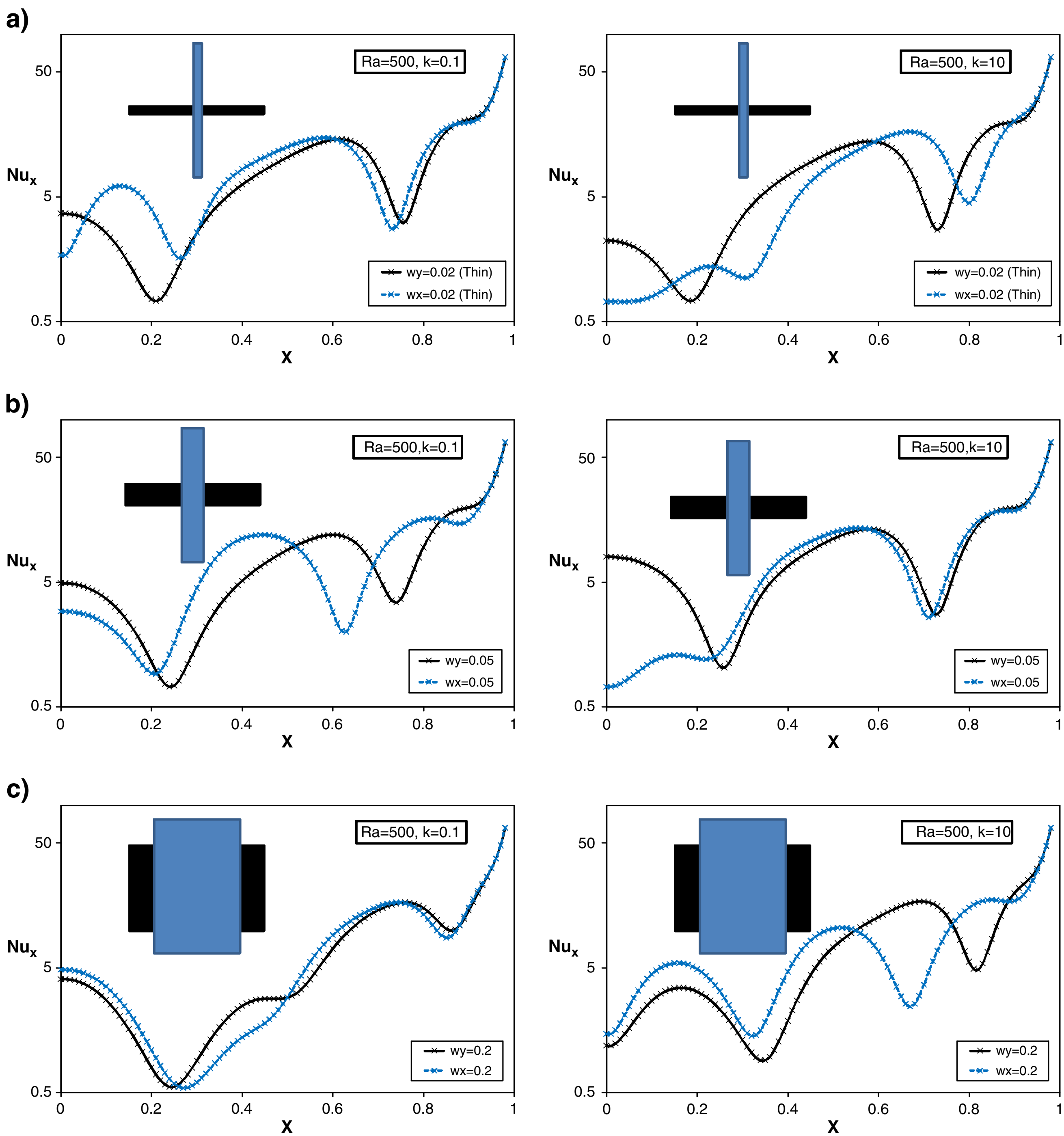

Fig. 7. The variation of the local Nusselt number along the horizontal bottom wall for different widths and heights of the conducting body at $k = 0.1$(left), $k = 10$(right) and $Ra = 500$: a)$wx = 0.02$, $wy = 0.02$, b)$wx = 0.05$, $wy = 0.05$, c)$wx = 0.2$, $wy = 0.2$.

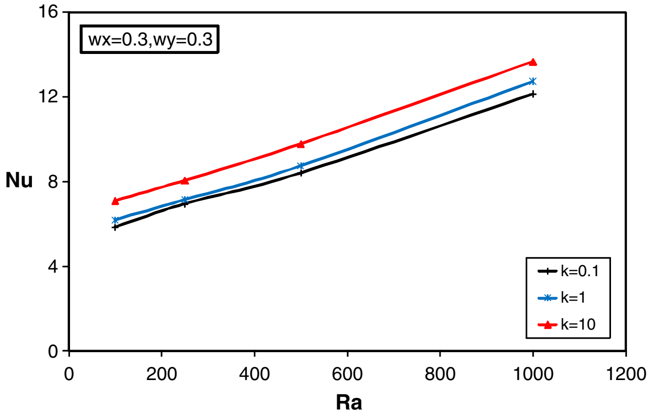

Fig. 8. The variation of the mean Nusselt number with the Rayleigh number for different thermal conductivity ratios at $wx = 0.3$, $wy = 0.3$.

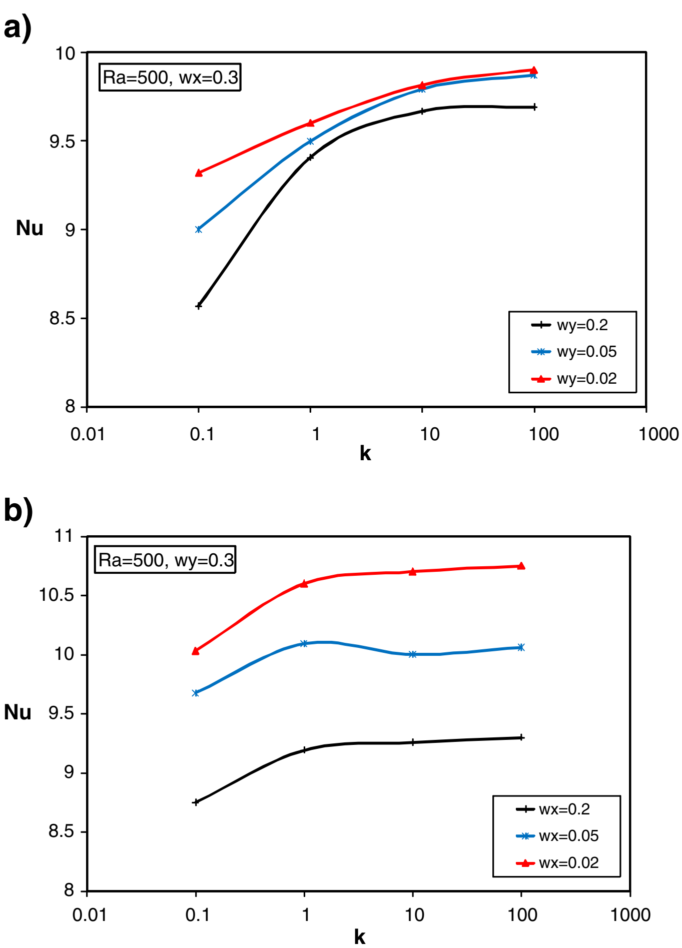

Fig. 9. The variation of mean Nusselt numbers with thermal conductivity ratio at $Ra = 500$: a) for different heights of the conducting body at $wx = 0.3$, b) for different widths of the conducting body at $wy = 0.3$.